Journal of Physics: Conference Series **160** (2009) 012044 doi:10.1088/1742-6596/160/1/012044

The Electromagnetic Calorimeter of CMS, Summary and Status

Werner Lustermann on the behalf of the CMS ECAL group

ETH Zurich, Institute for Particle Physics, ETH Hönggerberg, 8093 Zurich, Switzerland, c/o CERN, PH Department, 1211 Geneva 23

E-mail: werner.lustermann@cern.ch

Abstract. The construction of the lead tungstate crystal calorimeter for the CMS experiment at the Large Hadron Collider (LHC) is close to completion. The barrel part of the calorimeter composed of 61200 crystals is installed and operated inside CMS. Only 102 readout channels are problematic including the 21 entirely dead, corresponding to 0.17 % and 0.034 %, respectively. All 14648 end-cap crystals are mounted. The electronics installation and commissioning of one end-cap has finished and the second will be finished in few weeks. The construction of the pre-shower detectors installed in front of the end-caps is well advanced.

The many challenges of the design and construction imposed by a 4 Tesla magnetic field, radiation levels ranging from 100 krad up to several Mrad and a bunch crossing rate of 40 MHz were mastered by a huge effort in developing and testing appropriate crystals, photo-detectors and readout electronics carried out over the past ~ 15 years.
Test beam results demonstrate that the energy resolution obtained is better than 0.5 % at high energies. All readout channels in the barrel are inter-calibrated to better than 2 % using cosmic muons.

1. Introduction

The CMS experiment [1] is a typical collider detector, designed to study 14 TeV proton-proton collisions at the LHC with a bunch crossing rate of 40 MHz and a design luminosity of $10^{34}\,\mathrm{cm^{-2}s^{-1}}$. One of the primary goals is the discovery of the Higgs boson in the mass range suggested by precision electroweak measurements [2] of $m_H \leq 140\,\mathrm{GeV/c^2}$. Depending on the mass of the Higgs boson the $H \rightarrow \gamma\gamma$ and the $H \rightarrow W^+W^-$ with a subsequent identification of the W and Z bosons through their leptonic decay channels are the most promising discovery channels. In both cases a precise energy measurement for photons and electrons is mandatory. This can be achieved with a crystal calorimeter [3] [4].

2. Construction of the Calorimeter

The crystal calorimeter is made of 61200 lead tungstate crystals for the barrel and 14648 for the end-caps (see fig. 1). A fine-grained pre-shower detector is added in front of the end-cap calorimeter. Major design constraints are imposed by the operation in a 4 Tesla magnetic field and a high radiation environment.

The barrel calorimeter is made of two rings of 18 so called super-modules. Each of them covers 20° in ϕ and a pseudo-rapidity range up to 1.48. A super-module comprises 1700 crystals, of $\sim 26\,X_0$, arranged in four modules. Sub-modules of 2×5 crystals arranged in glass fiber supports,

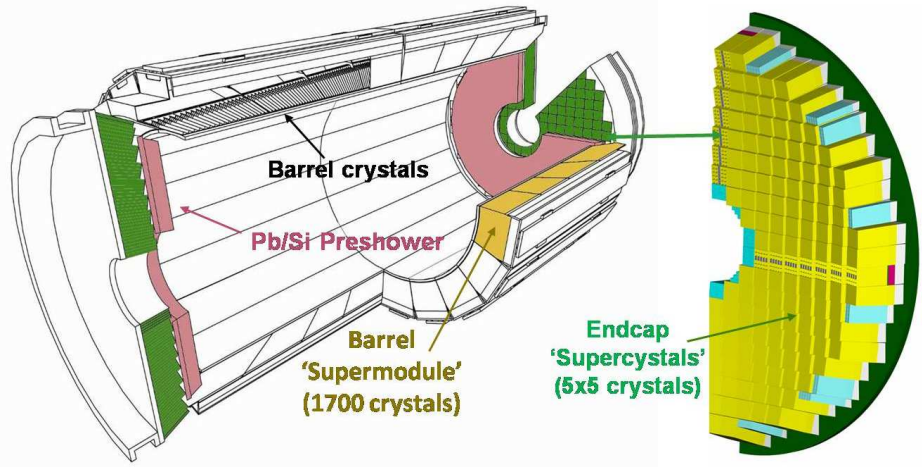

Figure 1. Schematic view of the CMS ECAL, including barrel, end-caps and pre-shower parts.

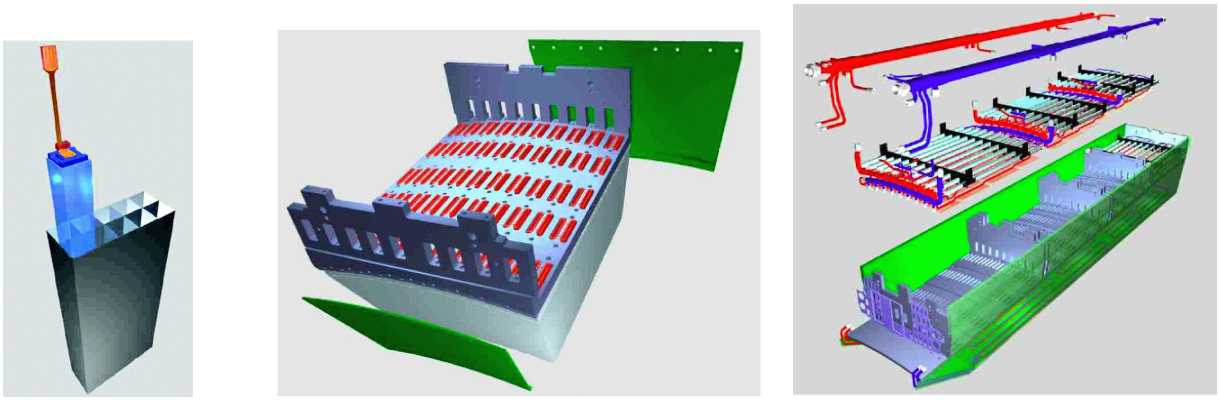

Figure 2. ECAL super-module assembly. Left : Alveolar structure during insertion of the first crystal; Centre : Complete module; Right : Expanded view of a super-module with cooling circuits.

the alveolar structures, together with their photo-detectors are the basic building blocks of the modules (see fig. 2). Hermeticity is achieved by an off-pointing geometry, obtained by a tilt of $\sim 3^\circ$ in η and ϕ of the crystals with respect to the interaction point.

The two end-caps consist of four so called "Dees" each made of 3662 crystals of identical shapes with $\sim 25\,X_0$ in length. Assemblies of 5×5 crystals together with their photo-detectors are arranged into alveolar structures forming so called super-crystals (SC) subsequently mounted onto one side of the Dees backplane (see fig. 3). The readout electronics and cooling circuits are attached to the opposite side. In total 156 SCs are mounted on a Dee. Eighteen of them are of special shape composed of less than 25 crystals in order to approximate the circular shape of the end-cap.

The pre-shower detector [5] is composed of two orthogonal layers of silicon micro-strip detectors placed behind (2 and 1) X_0 of lead absorber, respectively, covering a pseudo-rapidity range of $1.65 < \eta < 2.6$. It improves the π°/γ discrimination. The 4300, 63 mm long silicon sensors with a strip pitch of 1.9 mm are arranged into 496 ladders. They cover a total area of $16.6\,\mathrm{m}^2$.

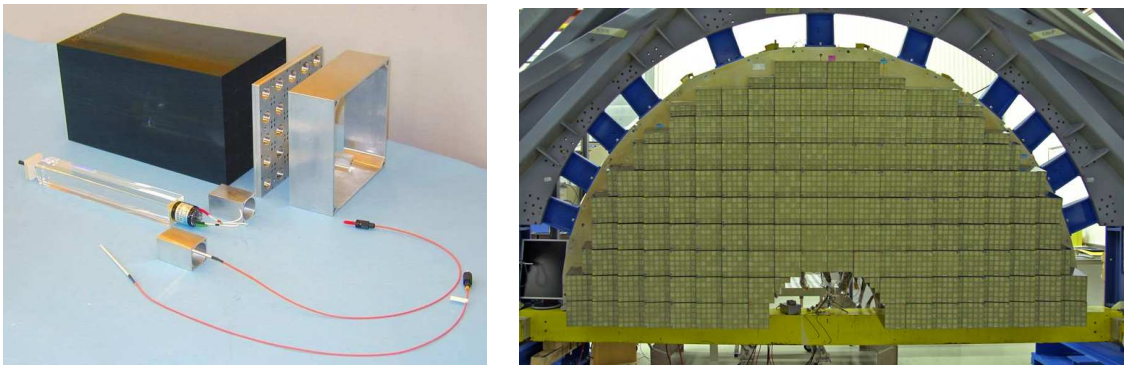

Figure 3. End cap construction: Left : Super crystal mechanics, crystal with VPT attached and monitoring fiber; Right : Dee backplane with all super-crystals mounted.

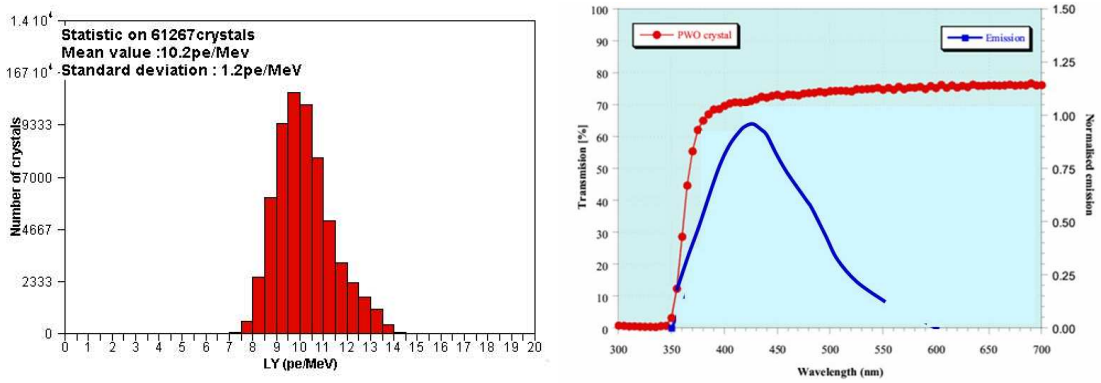

Figure 4. Light yield $PbWO_4$ (left). Transmission spectrum (red) and emmission spectrum (blue) of $PbWO_4$ crystals as a function of wavelength in nm.

3. Crystals

Lead Tungstate ($PbWO_4$) crystals were chosen for having a suitable combination of their properties. They have a short scintillation light decay time; in 25 ns $\sim$ 80% of the light is collected, a short radiation length of 0.89 cm and a small Molière radius of 2.19 cm. The light yield (LY) for 63000 crystals is shown in figure 4 [6]. Crystals with LY $<$ 8 p.e./MeV were rejected. The LY varies with $-2\,\%/°\mathrm{C}$ requiring a very stable temperature. Figure 4 shows the emission and transmission spectrum of lead tungstate. The emission maximum is at 430 nm. The measured light transmission is $(69.2 \pm 2.3)\,\%$ [7]. The required radiation hardness of the crystals has been achieved by doping them with Y/Nb, optimizing the crystals growth and stoichiometric fine tuning. The only radiation damage is a reduced light transmission. Low dose rate irradiations at 0.15 Gy/h were performed up to total doses of 1.5 Gy. Crystals with LY loss larger than 6% were rejected.

4. Photo-detectors

Because of the low light yield of the $PbWO_4$ crystals photo-detectors with intrinsic gain are required. Standard photo-tubes do not work in the 4 T solenoid field.

In the barrel calorimeter Avalanche Photo-Diodes (APDs) with an active area of $(5 \times 5)\,\mathrm{mm}^2$ are used. They were specially developed by Hamamatsu Photonics in collaboration with CMS

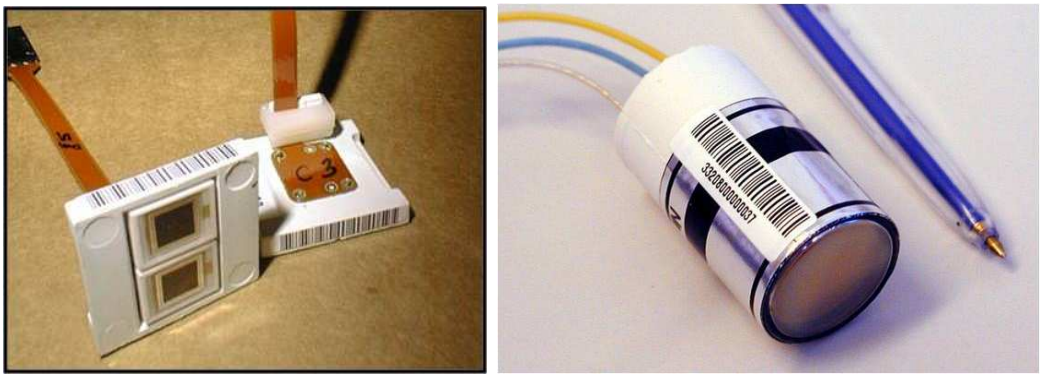

Figure 5. Capsules with two APDs and Kapton flex print (left), VPT (right)

(see fig. 5). The APDs are operated at gain 50 with a bias voltage of $(340 - 440)$ V. They have a capacitance of 80 pF, a quantum efficiency of 75% at 430 nm and an excess noise factor of 2 [8]. The gain depends on the bias voltage and on the temperature with 3.1%/V and $-2.4\%/\,^{\circ}$C, respectively.

The high radiation levels in the end-caps prohibit the use of APDs. Fortunately the angle between the photo-detectors and the magnetic field is limited to 24°. This allows the usage of Vacuum Photo Triodes (VPTs). The VPTs produced by RIE corporation in St. Petersburg have an active area of 280 mm^2 [9]. The quantum efficiency at 430 nm is 22%.

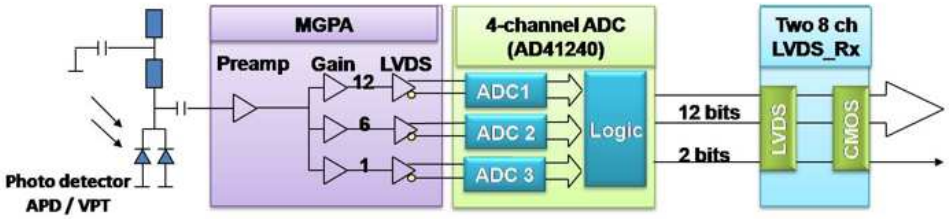

Figure 6. Schematic view of a single channel of the very front end electronics.

5. Readout electronics

The readout architecture of the ECAL is described in reference [10]. The on-detector electronics uses exclusively application specific integrated circuits. The Multi Gain Pre-Amplifier (MGPA) [11], amplifies and shapes the signal. In order to cope with the dynamic range of ~ 1.5 TeV, while maintaining the desired resolution of ~ 40 MeV three different gain ranges are implemented. The three outputs of the MGPA are digitized in parallel by a 4-channel, 40 MHz, 12-bit ADC, the AD41240 [12] and the data in the optimal gain range are selected (see fig. 6). Five identical channels are integrated in a very front end board together with output buffers. The digital data of 25 channels are stored in the so called front end (FE) card during the trigger latency. Every 25 ns the energy sum of 25 channels (barrel) or 5 channels (end-caps) is estimated and sent to the CMS trigger system using a 1 Gbit/s optical link. In case of a positive trigger decision the corresponding data are transferred using another Gbit optical link.

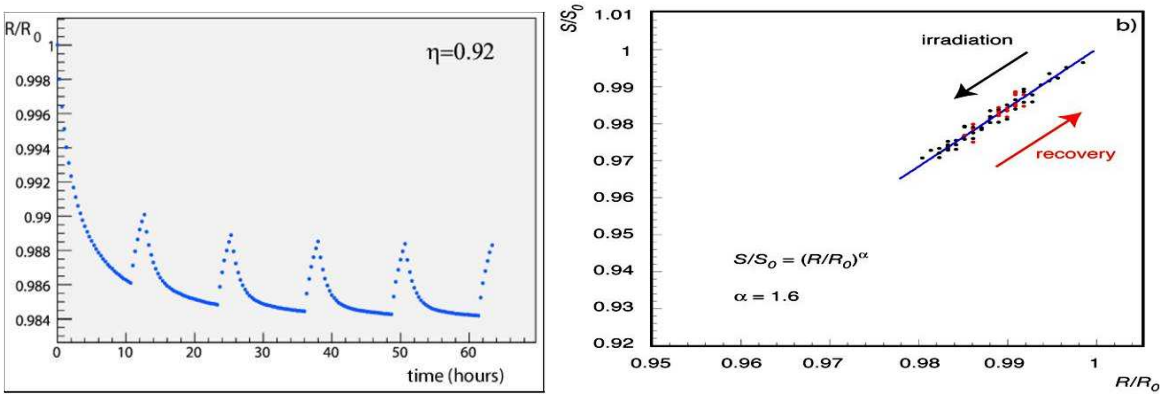

Figure 7. Simulation of the change of the crystal response to electrons due to irradiation (left). Measured correlation of the crystal response to 120 MeV electrons and to laser light (right).

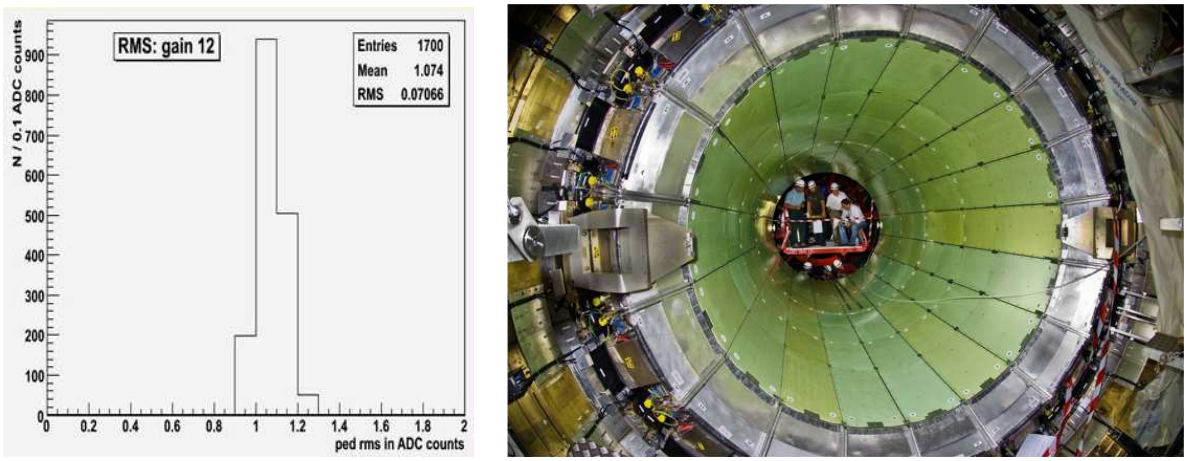

Figure 8. RMS of the pedestal in gain 12 for one super-module (left). All 36 barrel super-modules installed inside the CMS detector (right).

6. Light monitoring system

The calorimeter features a light monitoring system [13]. This is necessary because the light yield of the crystals varies with time due to radiation (see fig. 7). The light monitoring system injects light of two different wavelength, 440 nm and 700 nm into each crystal and measures the response. The correlation of the response of the crystals to laser light with respect to electrons was established during irradiation tests [14] (see fig. 7).

7. ECAL integration and installation

The integration of the ECAL electronics comprises the installation of almost 25000 printed circuit boards and about 8800 optical fibers [15]. Extensive testing at each installation step was mandatory. Therefore a dedicated ECAL electronics integration center was equipped with ECAL low and high voltage systems, cooling units, a detector control system, a laser system, dedicated special purpose readout systems and one final readout system. Originally designed for hosting three super-modules at a time finally up to six super-modules were accommodated simultaneously. The integration of the 36 barrel super-modules was completed within six months.

The performance of each readout channel was tested systematically during the installation. Figure 8 shows a typical distribution of the RMS of the pedestals of one complete super-module. The average noise of 1.1 ADC counts in gain 12 corresponds to $\sim 40\,\mathrm{MeV}$. Beside the measurements of the pedestals we used the test-pulse injection system of the MGPA and the laser monitoring system for systematic checks during integration and commissioning. The installation of the 36 barrel super-modules inside the CMS detector was completed in July 2007 (see fig. 8). Out of the 61200 installed channels only 102 (0.17 %) have problems including the 21 (0.034 %) which are entirely dead.

Since August 2007 the infrastructure has been adapted for super-crystal mounting and electronics integration of the four end-cap Dees. Two of them are complete and the remaining two will follow by end of July. Installation and test sequences are the same as in the barrel.

8. ECAL energy resolution and inter-crystal calibration

The energy resolution of the ECAL barrel super-modules was studied in detail during a test-beam period in summer 2004 [16][17]. The super-module was fully equipped with final readout electronics and connected to the final configuration of services including low and high voltage supplies, cooling system and temperature monitoring. Figure 9 shows the energy dependence of the energy resolution for a central $(4 \times 4)\,\mathrm{mm}^2$ impact of the beam into the crystal. Summing the energy in matrices of 3×3 crystals the obtained energy resolution for electrons of 100 GeV energy and higher is better than 0.5 %. A typical crystal has the following energy resolution for electrons entering the centre of the crystal:

$$\frac{\sigma_E}{E} = \frac{2.8\%}{\sqrt{E}} \oplus \frac{125\,\mathrm{MeV}}{E} \oplus 0.3\% \qquad (1)$$

As the energy is extracted by summing at least nine crystals, the relative calibration of the crystal readout channels is of primary importance. Main causes for different responses are the variation of the crystals light yield, the spread of the APD gains and the spread of the gains of the MGPAs.

While the final calibration is done in situ using data from π^0's, W and Z decays a good starting point is very desirable. Therefore nine of the 36 super-modules were calibrated using an electron beam [18], five with a beam energy of 90 GeV/c and four with a beam energy of 120 GeV/c. One of the super-modules was calibrated a second time one month after its first calibration. Figure 10 shows the distribution of the relative differences of the calibration constants. The measured

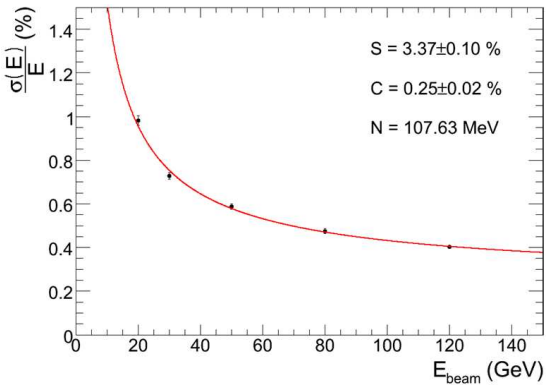

Figure 9. Energy resolution of a matrix of 3×3 crystals. The energy is reconstructed by summing the signals of the 3×3 crystals, for electrons entering the central $(4 \times 4)\,\mathrm{mm}^2$ area.

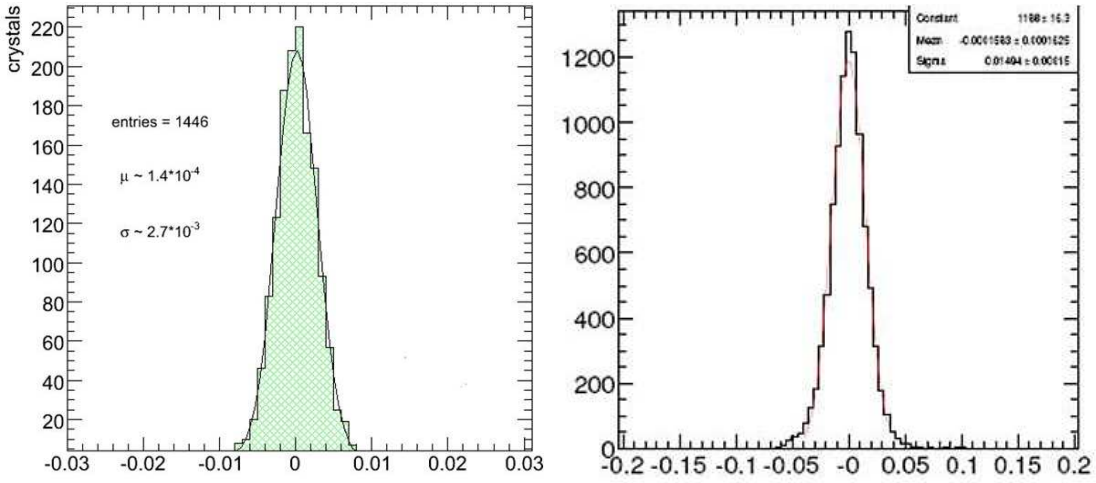

Figure 10. Relative difference of the calibration constants of two calibrations of one super-module (left). Relative difference of the calibration constants extracted from cosmic ray calibration and from electron beam calibration.

RMS of the spread is 0.27 % which is compatible with the statistical uncertainty obtained for the extraction of the calibration constants.

It was understood early enough that a calibration of all super-modules in an electron beam would not be possible. Therefore all 36 super-modules were calibrated with cosmic muon events. In order to assess the accuracy the relative difference of the calibration constants extracted from the cosmic muon calibration were compared with the results from the electron beam calibration. The spread depends on η ranging from 1.4 % to 2.2 % with an average of 1.5 % (see fig. 10) A similar inter-calibration of the four end-cap Dees was not possible, because of the tight schedule.

9. Summary and Outlook

CMS features a high resolution crystal calorimeter with an additional fine grained pre-shower detector in the end-cap region. The barrel part of the detector is installed inside CMS, commissioned and fully operational. It participates regularly to the CMS global data taking of cosmic muons. One of the two end-caps is ready for installation inside CMS and the second will follow soon. The pre-shower detector approaches completion. Systematic studies in an electron beam demonstrated an excellent energy resolution. Using cosmic muons and partially an electron beam a precise inter-calibration of all barrel crystals readout channels has been achieved. This will permit a fast understanding of the detectors in-situ calibration, mandatory for early physics results a the LHC.

10. Acknowledgment

First of all I would like to thank the organizers of the conference for the opportunity to present these results. It is also a great pleasure for me to thank the CMS ECAL group for their kind support in the preparation of the talk as well as of this report.

[1] "The Compact Muon Solenoid (CMS)", Technical Proposal, CERN/LHCC 94-38, LHCC/P1, 1994.
[2] The LEP Electroweak Working Group, "A Combination of Preliminary Electroweak Measurements and Constraints on the Standard Model", LEPEWWG/2003-01.

[3] G. L. Bayatian et al. "CMS The Electromagnetic Calorimeter Project-Technical Design Report", CERN/LHCC 97-33, 1997.
[4] G.L. Bayatian et al. "Detector Performance and Software, Physics Technical Design Report", Volume I, CERN/LHCC 2006-001
[5] E. Tournefier, "The Preshower Detector of CMS at LHC", NIM A461, pp. 355–360, 2001.
[6] E. Auffray et al. "Overview of the 63000 PWO Barrel Crystals for CMS ECAL production", IEEE Tans. in Nucl. Sci. vol 55, N03, June 2007,
[7] E. Auffray et al. "Status of the PWO Crystal production for the Electromagnetic Calorimeter of CMS and of its construction", Proceedings of the 7th International Conference on Inorganic Scintillators and Industrial Applications, SCINT2003, Valencia (Spain), 8-12 Sept. 2003, NIM A 537, pp 373-378, 2005
[8] Z. Antunovic et al. "Radiation Hard Avalanche Photo-diodes for the CMS Detector", 7th International Conference on Inorganic Scintillators and their Use in Scientific and Industrial Applications (SCINT 2003), Valencia, Spain, Sept. 2003, NIM A537, pp. 379-382, 2005.
[9] K.W. Bell et al. "The development of vacuum phototriodes for the CMS electromagnetic calorimeter", NIM A469, pp. 29–46, 2001.
[10] M. Hansen "The New Readout Architecture for the CMS ECAL", CERN-LHCC, pp. 78–82, 2003.
[11] M. Raymond et al. "The MGPA Electromagnetic Calorimeter Readout Chip for CMS", CERN-LHCC, pp. 83–87, 2003.
[12] G. Minderico et al. "A CMOS low power, quad channel, 12 bit, 40 MS/s pipelined ADC for applications in particle physics calorimetry", CERN-LHCC, pp. 83–87, 2003.
[13] J. Rander "The monitoring system for the CMS-ECAL", *Proceedings of the Eighth International Conference on Calorimetry in High Energy Physics*, Lisbon (Portugal), June 1999.
[14] A. Van Lysebetten and P. Verrecchia, "Performance and measurements of the light monitoring system for CMS-ECAL from 2002 test beam data", CMS NOTE, CMS RN 2004/001.
[15] W. Lustermann et al. "Installation and Test of the CMS Crystal Calorimeter Electronics", CERN-LHCC-2005-38.
[16] P. Adzic et al. "Energy resolution performance of the CMS electromagnetic calorimeter", CMS NOTE, 2006-140.
[17] P. Adzic et al. "Energy resolution of the barrel of the CMS Electromagnetic Calorimeter", CMS NOTE, 2006-148, JINST 2 P04004 (2007).
[18] P. Adzic et al. "Intercalibration of the barrel electromagnetic calorimeter of the CMS experiment at startup", CMS NOTE 2008/18.